



HAL
open science

Highly Structured 3D Electrospun Conical Scaffold: A Tool for Dental Pulp Regeneration

Lisa Terranova, Aurélien Louvrier, Anne Hébraud, Christophe Meyer, Gwenaël Rolin, Guy Schlatter, Florent Meyer

► **To cite this version:**

Lisa Terranova, Aurélien Louvrier, Anne Hébraud, Christophe Meyer, Gwenaël Rolin, et al.. Highly Structured 3D Electrospun Conical Scaffold: A Tool for Dental Pulp Regeneration. ACS Biomaterials Science and Engineering, 2021, 10.1021/acsbiomaterials.1c00900 . hal-03473464

HAL Id: hal-03473464

<https://hal.science/hal-03473464v1>

Submitted on 1 Dec 2022

HAL is a multi-disciplinary open access archive for the deposit and dissemination of scientific research documents, whether they are published or not. The documents may come from teaching and research institutions in France or abroad, or from public or private research centers.

L'archive ouverte pluridisciplinaire **HAL**, est destinée au dépôt et à la diffusion de documents scientifiques de niveau recherche, publiés ou non, émanant des établissements d'enseignement et de recherche français ou étrangers, des laboratoires publics ou privés.

Highly structured 3D electrospun conical scaffold: a tool for dental pulp regeneration

Lisa Terranova^{1,2}, Aurélien Louvrier^{3,4}, Anne Hébraud², Christophe Meyer³, Gwenaël Rolin^{4,5}, Guy Schlatter², Florent Meyer^{1,6}*

1. Université de Strasbourg, Institut National de la Santé et de la Recherche Médicale, Unité mixte de recherche 1121, Biomaterials and Bioengineering, Strasbourg, France

2. Université de Strasbourg, Institut de Chimie et Procédés pour l’Energie, l’Environnement et la Santé ICPEES UMR 7515, CNRS, Strasbourg, France

3. Service de chirurgie maxillo-faciale, stomatologie et odontologie hospitalière, CHU Besançon, F-25000 Besançon, France.

4. Université Bourgogne Franche-Comté, INSERM, EFS BFC, UMR1098, RIGHT Interactions Greffon-Hôte-Tumeur/Ingénierie Cellulaire et Génique, F-25000 Besançon, France ;

5. Inserm CIC-1431, CHU Besançon, F-25000 Besançon, France

6. Pôle de médecine et chirurgie bucco-dentaires, Hôpitaux Universitaires de Strasbourg, Strasbourg, France.

KEYWORDS

Tissue engineering, dental pulp regeneration, electrospinning, cell homing, dental pulp stem cells

ABSTRACT

New procedures envisioned for dental pulp regeneration after pulpectomy include cell homing strategy. It involves host endogenous stem cells recruitment and activation. To meet this cell-free approach, we need to design a relevant scaffold to support cell migration from tissues surrounding the dental root canal. A composite membrane made of electrospun poly(lactic acid) (PLA) nanofibers and electrospayed polycaprolactone (PCL) with tannic acid (TA) microparticles that mimics the architecture of extracellular matrix was first fabricated. After rolling the membrane in the form of a 3D conical scaffold and subsequently coating it with gelatin, it can be directly inserted in the root canal. The porous morphology of the construct was characterized by scanning electron microscopy (SEM) at the different length scales. It was shown that TA was released from the 3D conical scaffold after 2 days in PBS at 37°C. Biocompatibility studies were first assessed by seeding human dental pulp stem cells (DPSC) on planar membranes coated or not with gelatin to compare the surfaces. After 24 hours, results highlighted that the gelatin-coating increased the membrane biocompatibility and cell viability. Similar DPSC morphology and proliferation on both membrane surfaces were observed. The culture of DPSC on conical scaffolds showed cell colonization in the whole cone volume, proving that the architecture of the conical scaffold was suitable for cell migration.

1. INTRODUCTION

Root canal treatment is a common procedure to treat irreversible damages to a dental pulp by infectious disease or trauma. Such a procedure has a failure rate of 10 to 20 % marked by occurrence of an infection that jeopardizes tooth conservation. In addition, even if successful, such a procedure no longer allows the tooth to respond biologically to any future aggression, shortening thus the lifespan of the tooth. So for several years, the treatment paradigm of pulp disease tends to move to a more conservative approach. Conservation or restoration of pulp vitality is a goal to ensure preservation from reinfection or fracture. These approaches are based on the concepts from regenerative medicine. Currently, *revascularization* procedures are

promisingly used to repair immature teeth with necrotic pulp or apical periodontitis.¹ *Revascularization* relies on the complete disinfection of the root canal and the initiation of intra-canal bleeding. It results in pulp-like tissue formation, deposition of newly dentin, root lengthens and foramina closing.^{2,3} More recently, researchers transposed this strategy to mature teeth^{4,5} paving the way to regenerative endodontics. The emergence of tissue engineering has opened possibilities with concepts as cell seeding or cell homing using dedicated scaffolds to test dental pulp regeneration.

Cell homing is a relatively new clinical strategy based on the active recruitment of host endogenous cells by the chemotactic effects of signaling molecules into an anatomic compartment.⁶ Application to dental pulp regeneration sounds viable because stem cell niches are present close to the dental root in the periodontal ligament and the alveolar bone.^{7,8} Chrepa *et al.* found that evoked bleeding delivered mesenchymal stem cells (MSC) from the bone marrow into the root canal of mature teeth with apical lesions.⁹ It was established that dentin matrix is a source of bioactive molecules that can attract stem cells by chemotaxis, promote their differentiation into odontoblast-like cells and induce mineralization of newly dentine.^{10,11} Such bioactive molecules, like TGF- β , PDGF, bFGF, VEGF, or BMP-1 are found to be released by dentine surface conditioning with ethylenediamine tetraacetic acid (EDTA) or can be released from the blood clot after evoked bleeding.^{12,13} Several studies showed positive results of pulp-like tissue regeneration through chemotaxis-induced cell homing.¹⁴ The healing success via endogenous cell homing relies as well on the perfect intra-canal preparation and disinfection.

Studies on regenerative endodontics showed that scaffold implantation is needed to ensure tissue ingrowth on the entire length of the root. Scaffold has to provide a biological 3D micro-environment that can support cell attachment and growth.^{15,16} Among the range of biomaterials used for tissue engineering applications, nanofibrous scaffolds are gaining in popularity: as they

mimic the native extracellular matrix and serve as a 3D template with interconnected porosity and high surface area allowing cell adhesion, spreading, and differentiation.¹⁷ They were synthesized by various techniques including electrospinning, molecular self-assembly, and thermally induced phase-separation.¹⁸ Electrospinning is a versatile process enabling the production of continuous nano- or micro-fibers from a natural and/or synthetic polymer solutions subjected to a high electric field. It has been demonstrated that electrospun nanofibrous scaffolds can promote *in vitro* cell attachment, proliferation, and differentiation of dental pulp stem cells (DPSC)^{19,20} or periodontal ligament stem cells (PDL).²¹ Nanofibrous scaffolds have the potential for surface functionalization with bioactive molecules^{19,22} and/or antibiotics.²³ However, the simple electrospinning method leads to a scaffold with small pores of few microns which could inhibit adequate cellular infiltration and colonization.²⁴ Scaffolds with much larger pores can however be achieved using the so-called “electrostatic template-assisted deposition” (ETAD).²⁵ ETAD strategy allows the controlled deposition of electrospayed microparticles above electrospun nanofibers previously deposited on a patterned collector made of well-designed protuberances. During ETAD, the charged electrospun nanofibers form a template with attractive columbic forces above the fiber strands in direct contact with the protuberances of the collector as well as repulsive columbic forces above the fiber strands suspended between protuberances. This electrostatic template is then able to guide the deposition of electrospayed microparticles above the attractive areas at the top of the protuberances of the collector. If layers of nanofibers and microparticles are successively deposited, then ETAD strategy allows the fabrication of 3D scaffolds with pores of controlled size in the range of tens to few hundreds of microns using various kinds of materials depending on the targeted application.

Numerous scaffolds research for regenerative endodontics concerned injected materials as hydrogel.^{26–28} However, we strongly believe that a scaffold for dental pulp regeneration should

ideally be shaped in the form of a 3D tubular structure, as a cone similar to the dental pulp. Dental practitioners are commonly using “cone shape” material of a definite size that can be inserted to pre-determined length into the root canal and filled the entire space like gutta-percha point. So producing a 3D conical biomaterial shaped like a root canal would insure rapid use in clinical practice. For rapid and easy implantation, it must be sufficiently rigid to avoid material structure damage but also flexible to fit all shapes of root canals that can be curved. The cones could be produced in several diameters and lengths to adapt to different root canal anatomies. They should be easily handled by a dentist, stored in dental practices and cost-effective. For a cell homing based tissue engineering approach, the cone once implanted should be able to support evoked bleeding, migration and ingrowth of stems cells over the material as for revascularization in immature teeth. Only few authors reported studies about implantable scaffolds with tubular and/or conical shape. Bottino *et al.* were the first to report the fabrication of a 3D tubular scaffold obtained from the electrospinning of polydioxanone (PDS), which could be introduced in the root canal system of immature teeth.²⁹ Later, Louvrier *et al.* worked on a conical electrospun scaffold made of polycaprolactone (PCL).³⁰ But these materials were not focused on porous architecture for cellular infiltration or can not be used for the regeneration of mature teeth.

The present study aims to design a 3D porous conical scaffold and validate its use for dental pulp tissue regeneration of mature teeth. Architecture of the developed scaffold is major as the planned strategy for regeneration relies on cell homing. Scaffold should be enough porous to allow cell migration and vascularization within. ETAD strategy was used in order to build a 3D structured scaffold with regularly distributed sparsely and dense fibrous areas. The membranes were then rolled in a conical form and subsequently coated with gelatin. Poly(lactic acid) (PLA) was used for the electrospun nanofibers as a suitable polyester dedicated for biomedical applications. The electrosprayed microparticles were elaborated with both PCL and tannic acid

(TA). PCL of low molar mass was chosen as an optimal biopolymer dedicated to electrospinning and tissue engineering applications. TA, a biocompatible polyphenol from plants, was added in the formulation of the microparticles due to its antibacterial properties.^{31,32} Finally, the behavior, migration and colonization of DPSC were studied to validate the architecture of the biomaterial and its potential use in regenerative endodontics.

2. MATERIAL AND METHOD

2.1 Preparation of PLA/PCL-TA membranes

PLA/PCL-TA membranes were prepared by the alternate electrospinning of PLA and electrospinning of PCL-TA. For electrospinning, PLA (Mw = 180 kg/mol, Ingeo 7000D, NatureWorks) was solubilized in a mixture (v/v 50/50) of dichloromethane (DCM, Sigma-Aldrich) and N,N-dimethylformamide (DMF, Sigma-Aldrich) at a concentration of 10% wt. For electrospinning, PCL (Mw = 14kDa, Sigma-Aldrich) was solubilized at a concentration of 10% wt in dimethylacetamide (DMAc, Sigma-Aldrich) and TA (Sigma-Aldrich) was added at a concentration of 30% wt relatively to the weight of PCL. A homemade electrospinning set-up was composed of 18G needles connected to high-voltage power supplies (Spellman SL 10) and a rotating mandrel connected to a negative high-voltage power supply (Spellman SL 10). A patterned collector (100 x 40 mm), 3D printed (Silex 3D print, Thizy-les-Bourgs, France), was fixed on the mandrel for alternating collection of PLA fibers and PCL-TA particles. The collector was composed of many circular protuberances with a diameter of 0.7 mm arranged in staggered rows. Polymer solutions were loaded into 10 mL plastic syringes controlled by syringe pumps (Fisher Scientific) at a given flow rate. For PLA electrospinning, the needle-to-collector distance was fixed to 18 cm, the needle was subjected to a voltage of 12 kV and a solution flow rate of 1.7 mL/h was imposed. For the PCL-TA electrospinning, three needles were placed around the collector at a distance of 18 cm from the collector and subjected to a

positive potential of 20 kV. The PCL-TA solution was delivered at a flow rate of 0.3 mL/h for each needle. A negative voltage of -0.5 kV was imposed to the collector with a rotation of 1 rpm. The scaffold collection time was 13 min. As ambient conditions influence electrospinning,³³ temperature was set at 23 ± 2 °C and relative humidity at $RH = 40 \pm 5$ %. The scaffold was then carefully peeled off the collector, dried, and placed under vacuum overnight to remove any residual solvent. For fluorescent microscopy, Nile Red (Sigma) was added to the PLA solution at a concentration of 5 µg/mL to obtain red fluorescent fibers.

2.2 Membranes shaping in the form of 3D conical scaffolds

PLA/PCL-TA membranes previously obtained were shaped in the form of 3D conical scaffolds to fill the root canal space. A conical scaffold was made of a superposition of 3 membranes which were cut using a trapezoidal pattern (parallel bases= 9 mm and 3 mm, height = 17 mm). The membranes were then wrapped around a finger plugger (Finger Plugger- Metal Handle- 25 mm- Size 20A, Ref: 671715, Dentsply Maillefer) to obtain cones of equivalent shape. The conical scaffolds were then treated during 30 seconds to plasma cleaner (Plasma cleaner PDC-32G-2, Harrick Plasma) to render the surface of the PLA fibers hydrophilic. Subsequently, the treated conical scaffolds were immersed for 5 seconds in a 1% gelatin solution (Gelatin from porcine skin, CAS number 90000-70-8, Sigma-Aldrich) to stabilize the shape process. The gelatinized cones were then placed at -80°C for 24 h before freeze-drying (CHRIST Alpha 1-4 LD plus lyophilizator, Martin Christ Freeze Dryers GMBH, Osterode am Harz, Germany) for another 24h.

To evidence the correct size of cones and their handling, they were put into the root canal of a prepared tooth. A cone was previously immersed in gelatin supplemented with 20% barium sulfate (Sigma) to make it radiopaque. Radiographs were taken using an intraoral X-ray machine (RXDC, MyRay, Italia).

2.3 Characterization of the scaffolds

2.3.1 Morphological characterization of PLA/PCL-TA membranes

The morphology of the membranes was characterized by SEM (Tescan VEGA III, Czech Republic) with an accelerating voltage of 5 kV. PLA/PCL-TA membranes were coated with a layer of gold by sputtering under vacuum (Q150RS, Quorum technologies, UK). The distribution of the fiber diameter was obtained from at least 300 measurements from SEM images using image analysis software (ImageJ 1.52h, NIH). Particle size was measured from SEM images using Image J from 50 particles. Area fraction (%) was determined from 50 images taken randomly on 5 membranes. Images were thresholded and the area fraction was calculated using Image J software. The calculation was performed by dividing the area of the pixels of the background threshold by the total number of pixels of the image. Area fraction from 2D images corresponds to the voids not covered by fibers.

The surface and cross-section of the 3D conical scaffolds were characterized by SEM (Quanta 250 FEG, FEI Company, Eindhoven, The Netherlands). Cones were coated with gold-palladium alloy using a Hummer JR sputtering device (Technics, CA, USA) and images were captured at 5 kV. For cross-section views, cones were cut to explore the internal architecture and the organization of the sheets of rolled membranes. Cones were frozen in liquid nitrogen for 5 min and immediately cut with a blade. A total of 10 cones were cut to measure the average diameters of the two ends (1 mm from the ends for a clean cut) and the average inner diameter. Measurements were done using Image J software.

2.3.2 *In vitro* gelatin dissolution and tannic acid release from PLA/PCL-TA membranes

Gelatin dissolution was assessed on 17 cm² membranes to detect it. First PLA/PCL-TA membranes were coated with gelatin to mimic the treatment of the cones (G@PLA/PCL-TA

membranes). They were immersed in 1% gelatin solution, frozen at -80°C for 24 hours before being freeze-dried for another 24h. G@PLA/PCL-TA membranes were incubated in 1 mL of PBS at 37°C until 10 days. Each day, the supernatant was collected and the concentration of proteins was quantified using a BCA proteins assay (BioRad protein assay kit 2, REF 5000002, Bio-Rad) following manufacturer instructions using a BSA solution for the standards.

The surface of G@PLA/PCL-TA membranes was observed by SEM as previously described. To characterize gelatin dissolution on surface, membranes were immersed in 1 mL of PBS at 37°C for 1 and 7 days before SEM observation (Supporting information).

Tannic acid release from particles was studied by immersing 2 cm^2 of PLA/PCL-TA and G@PLA/PCL-TA membranes in 1 mL of PBS at 37°C . From day 1 to day 10, the supernatant was collected and absorbance was read at 270 nm on a spectrofluorometer (SAFAS FLX-Xenius, Monaco). TA quantification was done using a standard curve made in PBS.

2.3.3 3D conical scaffolds degradation

Degradation of the 3D conical scaffolds overtime was performed by immersing cones in 1 mL of PBS (pH= 7,4) at 37°C until 120 days. The pH values of PBS with cones were measured regularly using a micro pH electrode (pH electrode InLab Micro, Mettler Toledo) and compared to 1 mL of PBS at 37°C . In parallel, weight measurements were done several times until 120 days. Cones were pulled out PBS and dried for 1 week at 37°C to remove any traces of PBS.

To evaluate both inner and outer architecture of cones immersed in PBS at 37°C , cross-section and surface of the cones were observed at day 1, 7 and 15 and 120 by SEM in the same conditions as previously described.

Tannic acid release from cones was studied by immersing them in 1 mL of PBS at 37°C . The supernatant was quantified until 10 days.

All analyses were performed in triplicate.

2.4 Isolation of DPSC

DPSC were isolated from fresh pulp tissue extracted from human third molars from 1 donor after approval (CODECOH n° DC 2018-305). Extracted teeth were cleaned and cut longitudinally using a diamond bur under irrigation to expose the pulp chamber. Pulp tissue was gently removed and digested in a solution containing 2.5 mg/mL collagenase type I (Gibco, Ref 17100-017) and 4 mg/mL dispase II (Roche, Ref 04942078001) for 2h at 37°C. Then, the resulting solution was filtered on a 70- μ m cell strainer and the cells were collected following centrifugation. Cells were cultured in complete α -MEM (minimum essential medium, α modification) (Gibco) containing L-glutamine, 10% fetal bovine serum (FBS) (Gibco), 1% penicillin-streptomycin under a humidified atmosphere with 5% CO₂ at 37°C. The culture medium was refreshed every two or three days. Cells between passages 3 to 5 were used for all experiments.

2.5 Cytotoxicity test

Cytotoxicity of PLA/PCL-TA and G@PLA/PCL-TA membranes was studied by an indirect testing method based on ISO 10993-5 standards. Membranes with a surface of 6 cm² (ISO 10993-12) were cut and immersed in 1 mL of complete α -MEM medium under a humidified atmosphere with 5% CO₂ at 37°C for 24 hours. DPSC were seeded in a 96 well-plate at a concentration of 5×10^4 per well. After 24 hours, the standard medium was replaced by 100 μ L activated mediums in contact with membranes. Standard medium was used for negative control and 0,1% Triton X-100 (Sigma, Ref T8787) was used for positive control. Cytotoxicity was tested after 24 hours with an Alamar blue assay to measure the number of viable cells for each condition. Briefly, cells were incubated with 10% resazurin solution in each medium for 1h30 at 37°C. Supernatants were transferred in black 96-well plate and fluorescence was read with

an excitation wavelength at 560 nm and an emission wavelength at 590 nm (SAFAS FLX-Xenius, Monaco). The number of cells was calculated from a calibration curve. Analysis was performed in 5 samples for each condition.

2.6 DPSC culture on planar PLA/PCL-TA and G@PLA/PCL-TA membranes

Preliminary tests of cell culture were made on planar sheets for PLA/PCL-TA and G@PLA/PCL-TA membranes to test the surfaces. Before cell seeding, membrane sheets were treated during 30 seconds to plasma cleaner and fixed in CellCrown inserts for 24-well plate (CellCrown™24NX, Scaffoldex Oy, Ref Sigma: Z742381) corresponding to a surface of 58 mm². Membranes were coated or not with 1% gelatin solution: 60 µL of 1% gelatin solution was deposited on the stretched membranes to covered them before freezing at -80°C and freeze-drying as previously described (G@PLA/PCL-TA membranes). Then, all membranes were sterilized under UV light for 1h on each side before being placed in a 24-well plate for seeding. For each experiment, DPSC were seeded at a concentration of 2x10⁴ cells/mL on PLA/PCL-TA membranes, G@PLA/PCL-TA membranes, and on a tissue culture plate (TCP) as control.

2.6.1 Cell morphology

Cell morphology was analyzed after 1 and 7 days by SEM. Membranes were washed in 0.125 M cacodylate buffer and fixed with 2.5% glutaraldehyde in cacodylate buffer 50 mM for 2h30 at room temperature. They were dehydrated with a gradient of ethanol and desiccated with hexamethyldisilazane for 30 min. Membranes were then coated by sputtering with gold-palladium alloy using a Hummer JR sputtering device (Technics, CA, USA). Analysis was performed in triplicate.

2.6.2 Cell viability

Cell viability was assessed by a LIVE/DEAD™ Viability/Cytotoxicity Kit (Ref L3224, ThermoFischer scientific) after one day of culture. The cells/membrane constructs were gently rinsed with PBS before incubation with 7.5 μ M calcein-AM and 2.5 μ M ethidium homodimer-1 for 30 minutes at room temperature. The presence of viable cells (green fluorescence) and dead cells (red fluorescence) was observed with a fluorescent microscope (Nikon Eclipse TI-S, Japan). Five individual fields of view were imaged for each sample and the percentage of dead cells to live cells was calculated using Image J. Analysis was performed in triplicate.

2.6.3 Cell proliferation

Cell proliferation was analyzed on days 1, 3, 7, 10, and 14. At each time point, the number of viable and attached cells was determined by an Alamar blue assay. Briefly, cells were incubated with 10% resazurin solution in complete α -MEM for 1h30 with 5% CO₂ at 37°C. Supernatants were transferred in black 96-well plate and the fluorescence was read with an excitation wavelength at 560 nm and an emission wavelength at 590 nm with a spectrofluorometer. Cell number was calculated by the means of a linear calibration curve from 10³ to 10⁵ cells. Analysis was performed 5 times for each time point.

2.6.4 Cell differentiation

Odontogenic differentiation of DPSC on PLA/PCL-TA and G@ PLA/PCL-TA membranes was assessed by following ALP activity and mineralization as described by Wang *et al.*³⁴ Cells were cultivated 14 days in standard medium containing 50 μ g/ml ascorbic acid, 5 mM β -glycerophosphate, and 100 nM dexamethasone in complete α -MEM. DPSC, described as odontogenic differentiation medium at 37°C with 5% CO₂. Medium was refreshed every two or three days. Culture on TCP with odontogenic differentiation medium was used as positive control and culture on TCP with only standard medium was used as negative control. Analysis was performed in triplicate.

At days 7 and 14, alkaline phosphatase (ALP) activity was measured using the substrate 6,8-difluoro-4-methylumbelliferyl phosphate (DIFMUP, Molecular Probes). Briefly, cells were rinsed with PBS and lysed with 150 μ L of 1% Triton-X 100 in HBSS. Cell lysate was harvested and centrifuged at 5000 g at 4°C for 15 min. 50 μ L of supernatant was transferred in a black 96-well plate with 50 μ L of 200 μ M DIFMUP solution. Plate was incubated for 15 min at 37°C in the dark. Fluorescence was read at an excitation of 358 nm and emission at 450 nm. Fluorescence intensity was normalized to the total protein content of supernatants determined with Pierce™ BCA Protein Assay Kit (Thermo Scientific) following manufacturer's instruction.

At day 14, mineralization was determined by measuring calcium-phosphate deposition using a calcium colorimetric assay kit (Sigma-Aldrich). First after thorough rinsing of each well with 1 mL PBS, 500 μ L of 1M acetic acid was added and plate incubated at 4°C in order to solubilize calcium phosphate deposition. After an overnight incubation, 50 μ L of solution from each well were transferred in a 96-well plate. 90 μ L of the chromogenic reagent plus 60 μ L of calcium assay buffer were then added to each well. After 10 min incubation, the absorbance was read at 575 nm. The calcium content was calculated using a standard curve and normalized to the quantity of total proteins measured as described above.

2.7 Cell migration

To test the migration ability of DPSC through PLA/PCL-TA membranes, a transmigration assay was first performed through planar membranes. Five PLA/PCL-TA membranes stained with Nile Red were piled up and fixed in the CellCrown inserts. DPSC were seeded on the top of the scaffold (upper chamber) in α -MEM medium. In the lower chamber, the medium was supplemented with 10% FBS. After 14 and 28 days of incubation, cells were fixed in 4% paraformaldehyde in PBS for 20 min, washed with PBS, and stained with DAPI (Invitrogen) at

a concentration of 10 $\mu\text{g}/\text{mL}$ for 15 min. Samples were washed 4 times for 5 minutes prior to observation by confocal laser scanning microscope (LSM 710 microscope, Zeiss, Heidelberg, German).

2.8 Cell proliferation and colonization into the 3D conical scaffolds

Before cell seeding, the 3D conical scaffolds stained with Nile Red were sterilized in ethanol 70% for 15 min under UV light and hold at the bottom of a 6-well plate. The wells were previously coated with polyhydroxyethylmethacrylate (PHEMA) to avoid any cell adhesion. 100 μl of a 10^6 cells/mL solution were gently seeded on the surface and inside the cones with a needle (26G, 0.45x12mm, Terumo) on a 1 mL microsyringe (Terumo). DPSC were cultured for 7, 14, 21, and 28 days in complete α -MEM medium. At each time point, the number of cells was determined by an Alamar blue assay as previously described. The number of cells was calculated from a calibration curve. Then, cells were fixed in 4% paraformaldehyde for 20 min in PBS and washed with PBS. For histological analysis, the cones were deposited in molds, covered with Tissue-Tek® O.C.T.™ and subsequently frozen at -20°C for 24 hours. 16 μm sections were cut and counterstained with DAPI at a concentration of 5 $\mu\text{g}/\text{mL}$ for 15 min for confocal microscopy observation. Analysis was performed in triplicate.

2.8 Statistical analysis

Results were expressed as mean \pm SD. Statistical analysis was performed using Systat 13 (Systat Inc., San José, CA). Differences for TA release from PLA/PCL-TA and G@PLA/PCL-TA membranes, cell proliferation and cell differentiation were performed with a parametric two-way ANOVA test. For others results, differences were analyzed by a non-parametric ANOVA (Kruskall-Wallis) followed by the Conover-Inman test for all pairwise comparisons. Differences were considered significant when $p < 0.05$.

3. RESULTS

3.1 Characterization of the scaffolds

3.1.1 Characterization of planar PLA/PCL-TA membranes by SEM

SEM characterization of the PLA/PCL-TA membranes revealed that they were perfectly 3D structured (Fig. 1A) and built according to the topography of the collector (Fig. 1B). Three main distinct areas can be observed: (1) the first was thick nodes made of intertwined PLA nanofibers and PCL-TA microparticles deposited on the cylindrical protuberances of the collector (Fig. 1D) and (2) the second was thin and highly porous with few randomly organized PLA fibers nanofibers (Fig. 1E), (3) the third was made of aligned and stretched PLA nanofibers connecting neighboring nodes (Fig. 1F) Nodes and aligned fibers provided the mechanical cohesion to the entire structure.(Fig. 1F).

The PLA fibers were smooth and uniform, they had a unimodal diameter distribution with an average value of 798 ± 205 nm (Fig. 1C). The PCL-TA particles had an average diameter of 1.28 ± 0.28 μ m. Pores were in the form of interconnected voids between fibers, and porosity was measured as the area fraction from the 2D images with Image J. Average area fraction of zones with only random fibers was 60 ± 10 % (percentage of void) and zones with aligned fibers was 40 ± 10 % (percentage of voids).

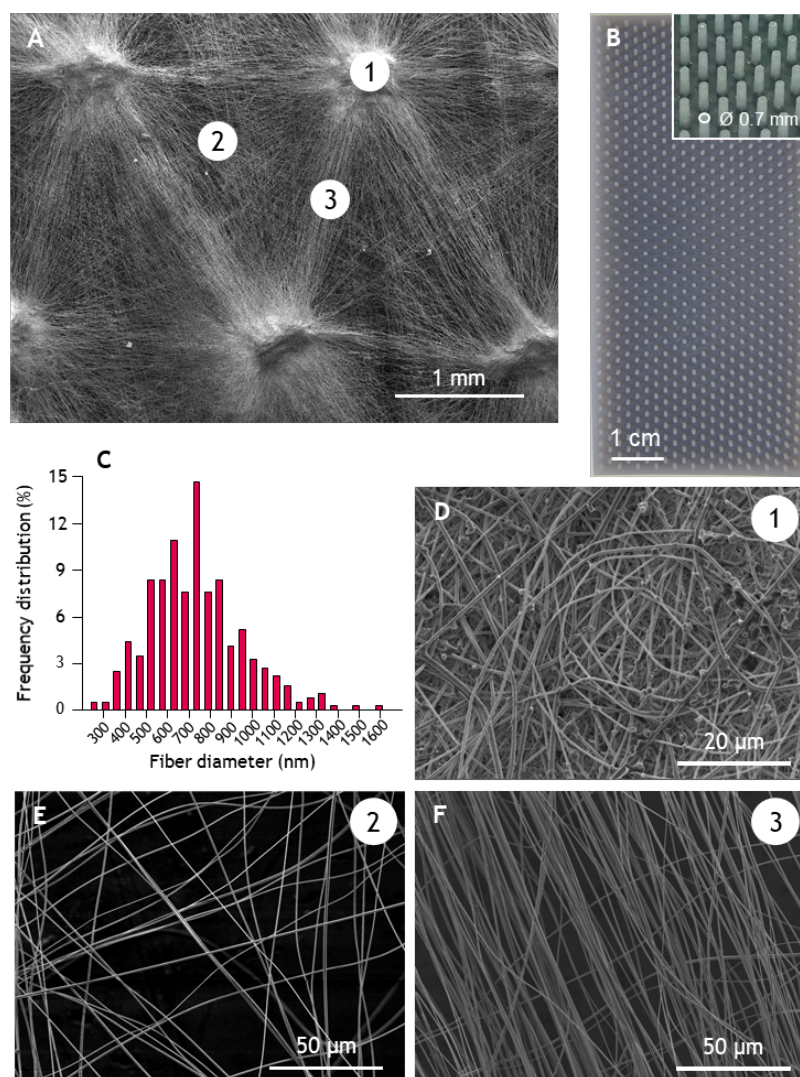


Figure 1: SEM observation of a structured PLA/PCL-TA membrane obtained by ETAD using a 3D printed patterned collector. (A) overall view of the membrane, it was well structured according to the topography of the patterned collector, (B) photograph of the patterned collector showing the regularly distributed protuberances, (C) diagram of fiber diameter distribution, (D) thick node composed of intertwined PLA fibers and PCL-TA microparticles located over a collector's protuberance in zone 1, (E) thin and porous area with a low density of randomly organized PLA nanofibers in zone 2, and (F) aligned PLA fibers connecting the nodes in zone 3.

3.1.2 Characterization of the 3D conical scaffolds

Standardized conical scaffolds, with a shape similar to a dental pulp canal after preparation for endodontic treatment, were fabricated from the structured PLA/PCL-TA membranes (Fig. 2A). Membranes sheets were rolled around a finger plugger and measured 17 mm long for comfortable manipulation. Six layers of sheet composed the cones, it was the ideal number of layers in terms of rigidity and flexibility for their insertion in prepared teeth. A cone around a finger plugger was put into the root canal of a prepared tooth. Radiograph showed that the cone had an adequate shape to fill the root canal (Fig. 2B).

The surface of the cones exhibited a layer of gelatin that covered the fibers (Fig. 2C). Cross-section of the 3D cones revealed that they had a circular and regular shape (Fig. 2D). The layers of membranes were perfectly rolled up on each other with some spaces between. The mean diameter of the tips of the cones was $477 \pm 81 \mu\text{m}$ while the largest end measured $975 \pm 199 \mu\text{m}$. The cone possessed a large tubular space at the center due to the rolling around the finger plugger. The average inner diameters of the tubular space were 316 ± 99 for the finest end and 552 ± 72 for the widest.

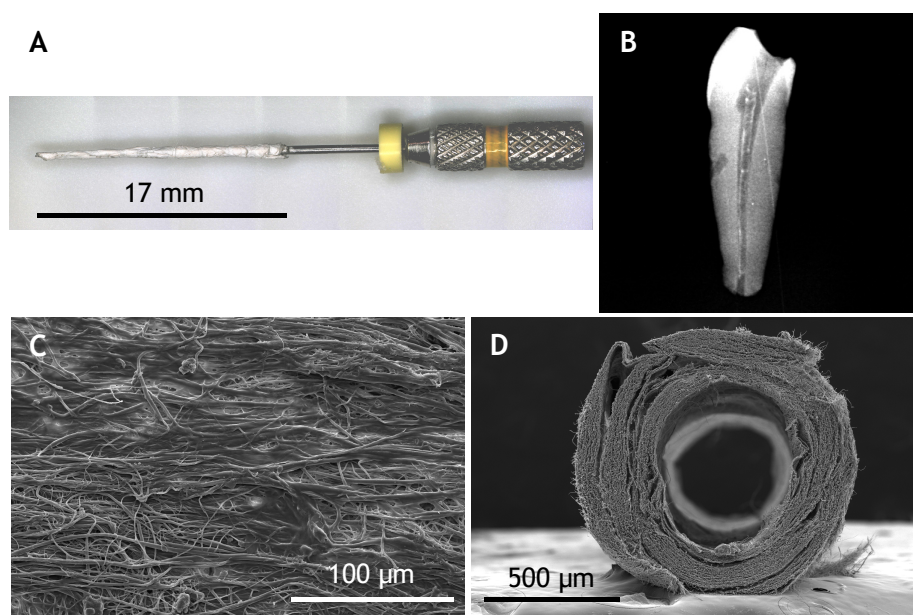


Figure 2: Characterization of the 3D conical scaffold. (A) Image of a cone taken with a Keyence digital microscope, (B) radiography of a cone filling a prepared root canal, (C) SEM of the surface of a cone after being coated with gelatin covering fibers, (D) SEM of the cross-section of a cone, note the circular shape made of layers of overlaid membranes. The large space at the center was due to the finger plugger used as support for the membrane rolling.

3.1.3 *In vitro* gelatin dissolution and tannic acid release

As non-crosslinked gelatin was used to avoid unwrapping the conical scaffolds, it is expected the progressive dissolution of gelatin coating over time. Gelatin release was studied on large sheets of PLA/PCL-TA membrane of 17 cm² previously coated with 1% gelatin solution. G@PLA/PCL-TA membranes were immersed in 1 mL of PBS at 37°C until 10 days and protein concentration in the supernatant was measured at day 1, 2, 3, 4, and 10. Results in Figure 3B presented the concentration of gelatin released after 10 days. Most of the gelatin (85%) was released on day 1. SEM observation of G@PLA/PCL-TA membranes immersed in PBS consolidated these results (Fig. 1SI). After 1 day, the coated layer of gelatin was already starting to dissolve whereas no trace of gelatin coating can be seen on day 7.

Tannic acid is known to be highly water soluble, incorporated in the PCL particles, it is not meant to react with PCL. The release of TA from PLA/PCL-TA and G@PLA/PCL-TA membranes was shown on Figure 3A. On day 1, the quantity of released TA was significantly higher from PLA/PCL-TA membranes compared to G@PLA/PCL-TA ones. Results showed that almost all TA (90% of total amount detected) was released from PLA/PCL-TA membranes against 72% for G@PLA/PCL-TA membranes. On day 2, released TA was significantly higher on the case of G@PLA/PCL-TA membranes (20% of the total amount detected after 10 days). Two days were necessary to release the same quantity of TA from G@PLA/PCL-TA membranes compared to the non-coated ones.

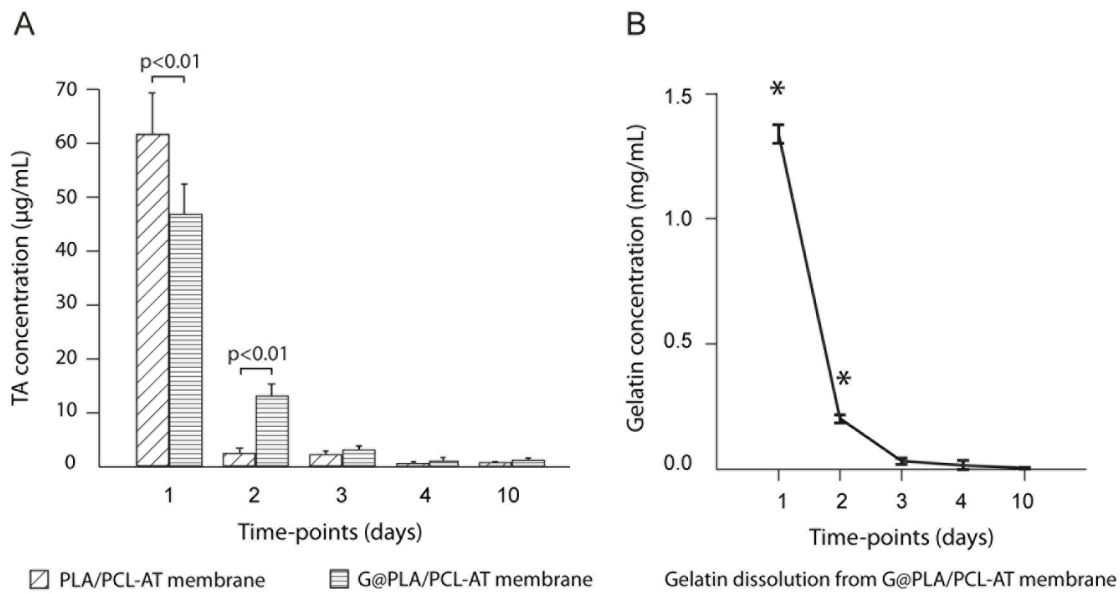


Figure 3: (A) Tannic acid release from PLA/PCL-AT and G@PLA/PCL-AT membranes immersed in 1 mL PBS at 37°C until 10 days, (B) gelatin dissolution from G@PLA/PCL-AT membranes until 10 days. Mean for $n = 3 \pm SD$. *Significant at $p < 0.05$.

3.1.4 3D conical scaffolds degradation

The mean concentration of released TA from the cones after 24 hours was 57.86 µg/mL corresponding to almost 60% of the total concentration detected after 10 days (Fig. 4A). After 72h, 89.65 µg/mL of TA was released corresponding to 92% of the total detected release, being 97 µg/mL, which took place after 10 days.

Membranes were made of biodegradable polyesters which are subject to hydrolysis over time leading to the progressive degradation of the material. This degradation was followed over 120 days. It was observed a slight decrease of the pH during the 120 days with no significant difference between PBS containing conical scaffolds or not (Fig. 4B). Starting from an average initial weight of 0.91 mg, the weight of the conical slightly decreased over the 120 days (Fig. 4C).

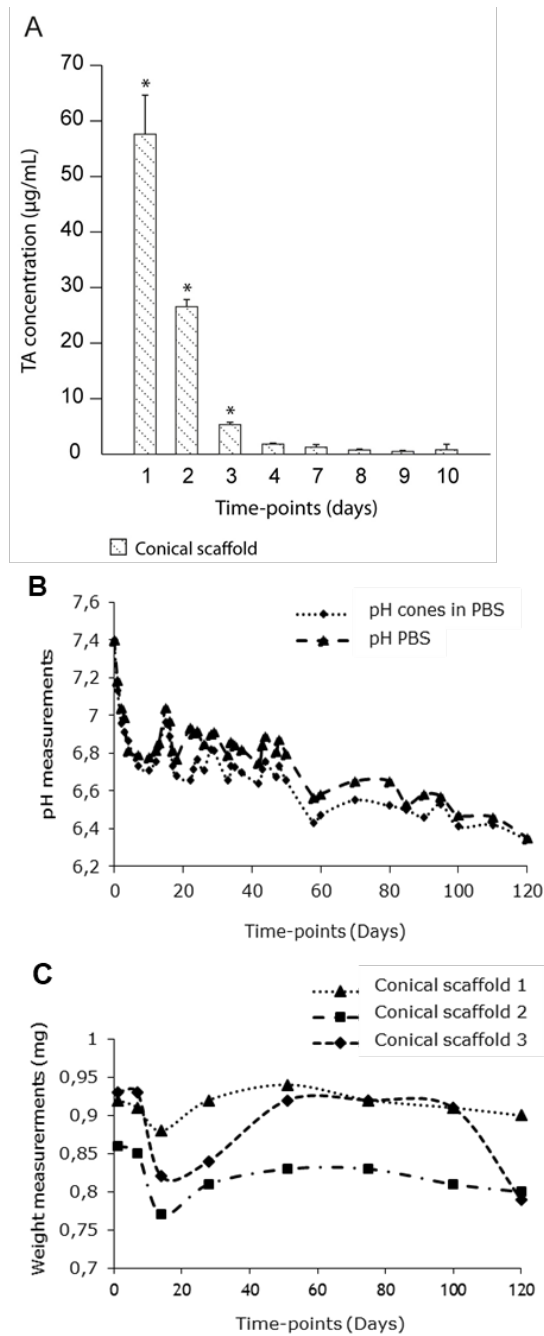


Figure 4: Cone degradation. (A) Tannic acid release from cones immersed in 1 mL PBS at 37°C until 10 days. Mean for $n=3 \pm SD$. *Significant at $p < 0.05$. (B) pH values ($n=3$) and (C) weight measurements of cones immersed in 1 mL PBS at 37°C over time until 120 days.

The morphology of cross-sections of the cones were explored by SEM on days 1, 7, 15, and 120. The cones kept their circular shape with an orderly stacking of layers until 7 days immersed in PBS (Fig. 5 A, B). After 15 days, the shape of the cone started to be deformed and loosened

but layers of membranes were still well stacked (Fig. 5C). After 120 days, the structure of the cone was extremely deformed and loosened (Fig. 5D). The SEM of the cone surface can be seen in Supporting information (Fig. 2SI).

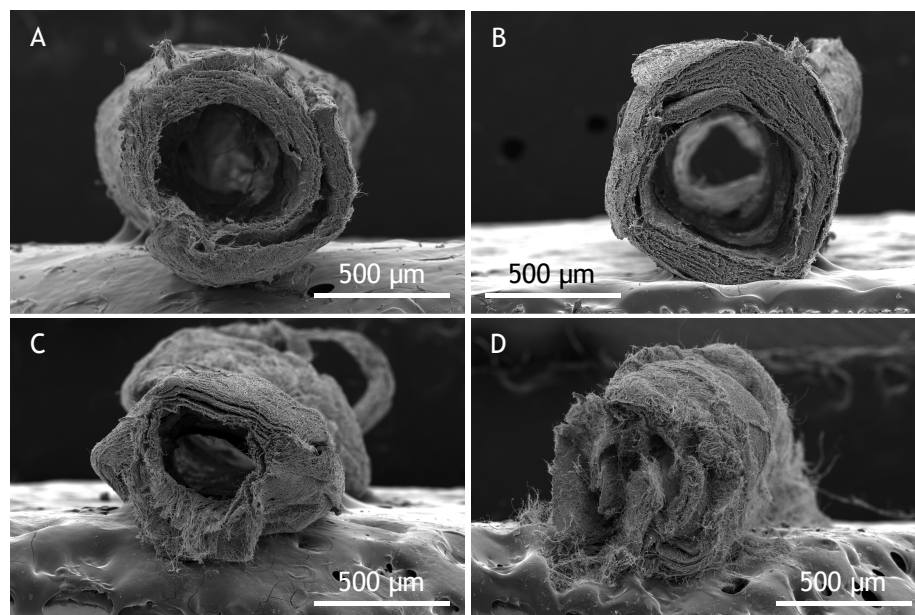


Figure 5: Cone degradation. SEM micrographs of cross-section of cones after (A) 1 day, (B) 7 days, (C) 15 days and (D) 120 days immersed 1 mL PBS at 37°C.

3.2 PLA/PCL-TA and G@PLA/PCL-TA membranes cytotoxicity

3.2.1 Indirect contact assay

The cytotoxicity of PLA/PCL-TA and G@PLA/PCL-TA membranes was first assessed using an indirect method as recommended by the ISO 10993-5 standard (Fig. 6). DPSC were cultured with medium activated in contact with membranes for 24 hours. For culture with medium activated with G@PLA/PCL-TA membranes, number of cells represented 72% of the number of cells with standard medium. According to ISO 10993-5, there is no toxicity of the G@PLA/PCL-TA membranes after 24 hours in accordance with cell viability limit fixed at

70% to the control. For cell cultured with activated medium with PLA/PCL-TA membrane, number of cells was below 70% of the number of cells cultured with standard medium.

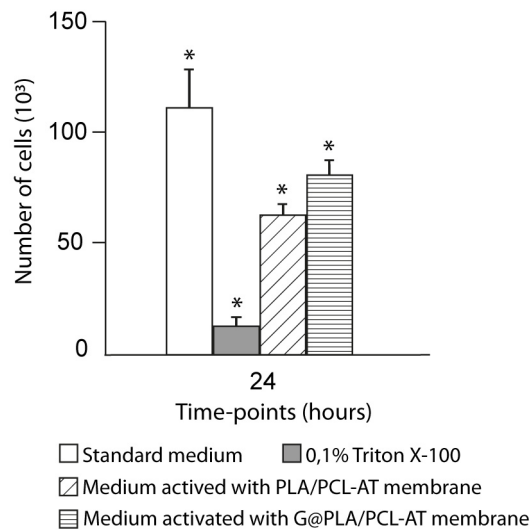


Figure 6: Cytotoxicity of PLA/PCL-TA and G@PLA/PCL-TA membranes. Activated mediums were prepared by incubating both membranes in 1 mL standard medium. Quantity of 5×10^4 DPSC per well were seeded 24 hours prior to cytotoxic assay. An Alamar blue assay was carried out 24 hours after refreshed medium. Standard medium was used as negative control and 0.1% Triton X-100 as positive control. Mean for $n = 5 \pm SD$. * Significant at $p < 0.05$.

3.2.2 Direct contact assay

The viability of DPSC deposited on PLA/PCL-TA and G@PLA/PCL-TA membranes was analyzed with a Live/Dead assay after 24 hours (Fig. 7). PLA/PCL-TA membranes showed mild direct toxicity on DPSC (76% of living cells) while gelatin coating on G@PLA/PCL-TA membranes significantly prevents this effect (92% of cell viability). Therefore, the G@PLA/PCL-TA membranes were considered as non-cytotoxic, as they did not show any statistical difference with cells cultured on TCP surface.

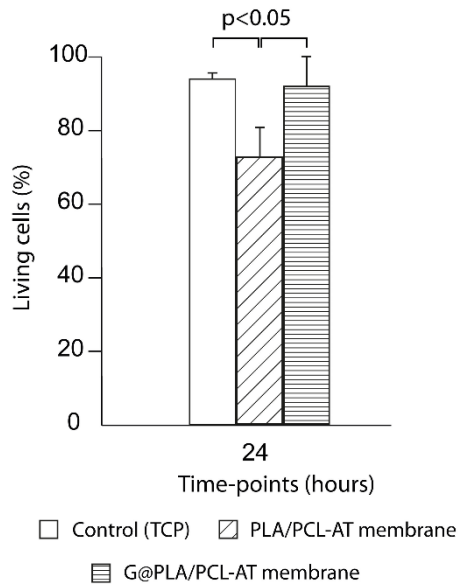


Figure 7: Viability of DPSC cultured on TCP (control), PLA/PCL-TA and G@PLA/PCL-TA membranes. Percentages of viable DPSC after 24 hours were calculated from five images per sample with Image J. Mean for $n = 3 \pm SD$.

3.3 Analysis of PLA/PCL-TA and G@PLA/PCL-TA membranes as cell culture surfaces

3.3.1 Cell morphology

Morphology of DPSC was observed by SEM after 1 and 7 days on PLA/PCL-TA and G@PLA/PCL-TA membranes (Fig. 8). Cells were uniformly spread and elongated on both membrane surfaces. On PLA/PCL-TA membranes, cells were located above and below fibers at days 1 and 7 (Fig. 8A, B). On day 1, cells cultured on G@PLA/PCL-TA membranes were above the fibers, and were attached to gelatin and the fibers sticking out (Fig. 8C). On day 7, gelatin was dissolved and cells were started to grow below fibers (Fig. 8D).

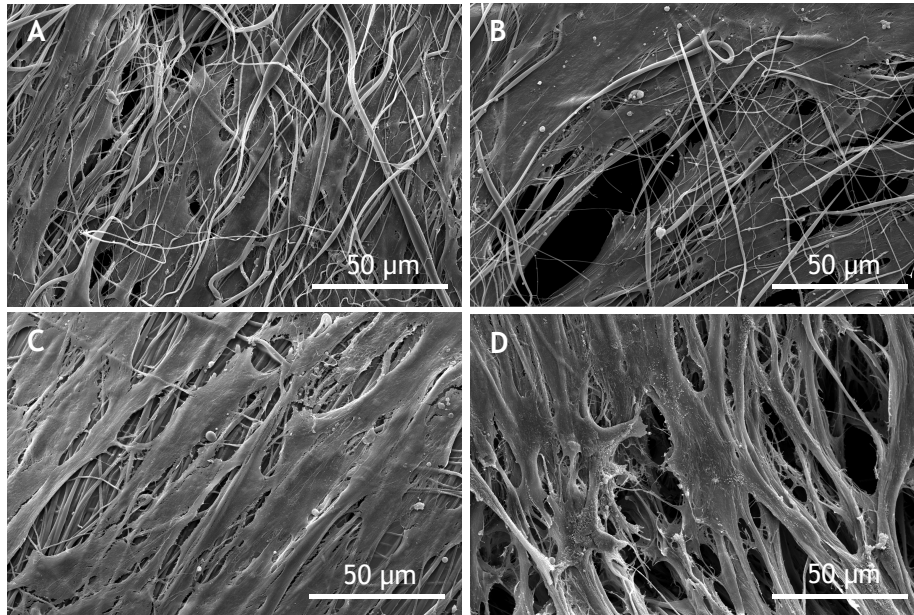


Figure 8: Morphology of DPSC. SEM of DPSC cultured on PLA/PCL-TA membranes after (A) 1 day, (B) 7 days. SEM of DPSC cultured on G@PLA/PCL-TA membranes after (C) 1 day, (D) 7 days.

3.3.2 Cell proliferation

DPSC proliferation was assessed by an Alamar blue assay at days 1, 3, 7, 10, and 14 (Fig. 9). Cell proliferation was recorded on each surface for up to 10 days. All data showed that the proliferation profile depends on the substrate. For both membranes, the proliferation was comparable to the control surface until 3 days. On G@PLA/PCL-TA membranes, cell proliferation was slower with a lag time between 3 to 7 days. On day 7, cell number was significantly comparable between PLA/PCL-TA membranes and TCP compared to G@PLA/PCL-TA membranes. On day 10 and 14, number of cells was significantly higher on TCP surface with no difference of proliferating cells between both membranes.

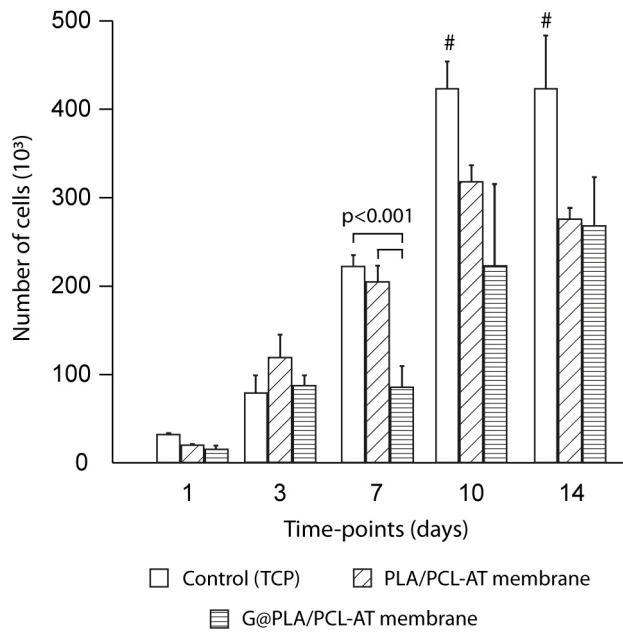


Figure 9: Proliferation of DPSC seeded on TCP (control), PLA/PCL-TA and G@PLA/PCL-TA membranes after 1, 3, 7, 10 and 14 days. Number of cells was assessed with an Alamar blue assay. The initial concentration of cells seeded was 2×10^4 cells/mL. Mean for $n = 5 \pm SD$. #Significant at $p < 0.01$.

3.3.3 Cell differentiation

To evaluate DPSC odontogenic differentiation on PLA/PCL-TA or G@PLA/PCL-TA membranes, ALP activity was measured at day 7 and 14 as shown in Figure 10A. At day 7, cells cultivated in odontogenic differentiation medium on PLA/PCL-TA or G@PLA/PCL-TA membranes had significantly higher ALP activity than negative control cells and comparable to positive control cells. However, DPSC cultivated on G@PLA/PCL-TA membranes showed slightly less ALP activity than positive control cells. The same observation was done on day 14 with an overall decrease in ALP activity in all samples cultivated in odontogenic differentiation medium.

Aside, amount of calcium-phosphate deposition, sign of mineralization, was measured after 14 days and showed similar results (Fig. 10B). All DPSC cultivated in differentiation medium showed an increase in calcium measurements compared to negative control cells. Altogether those results showed that DPSC reacted the same, no matter the surface was and therefore the material did not impede differentiation process.

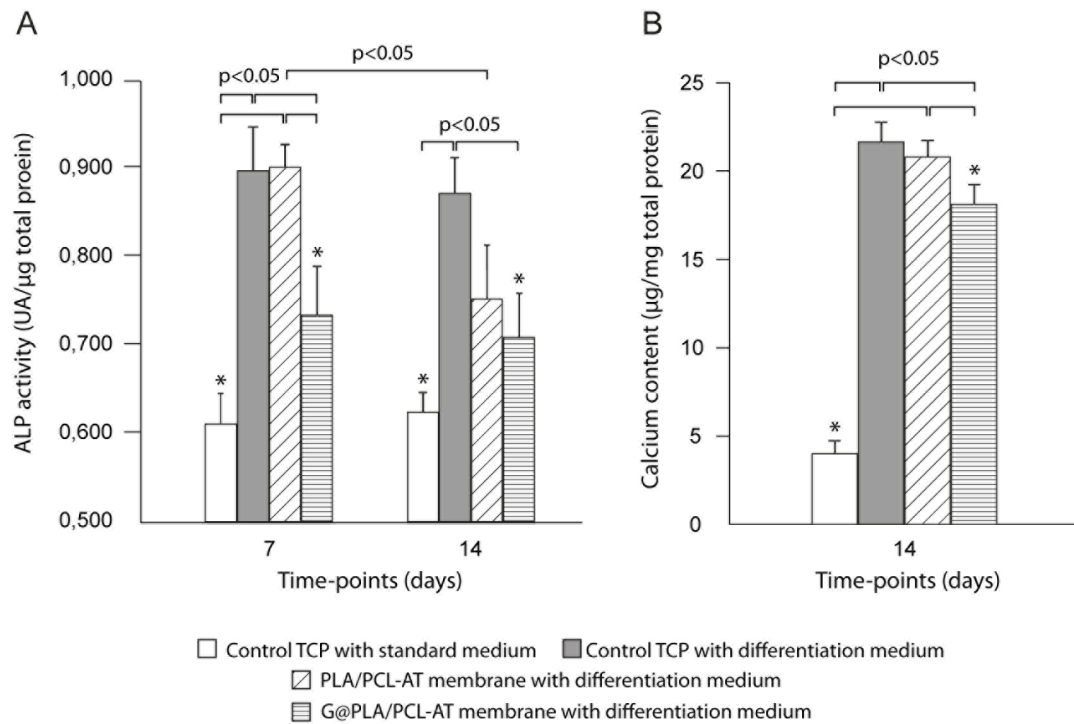


Figure 10: Odonto/ostogenic differentiation of DPSC cultured on TCP with standard medium and on TCP, PLA/PCL-TA and G@PLA/PCL-TA membranes with differentiation medium. (A) ALP activity of DPSC after 7 and 14 days, (B) calcium content measured after 14 days. The initial concentration of cells seeded was 2×10^4 cells/mL. Mean for $n = 3 \pm SD$. *Significant at $p < 0.05$.

3.4 Cell migration

Cell migration was analyzed by confocal microscopy 14 and 28 days after seeding on the top of five piled-up PLA/PCL-TA membranes. Z-stack images of $4 \mu\text{m}$ thickness were compiled

to a 3D image to observe cell location (DAPI) into the whole structure (Nile Red). Scaffolds were 120 μm thick. After 14 days, the cells had penetrated to a maximum depth of 50 μm (Fig. 11A). After 28 days of culture, cells had migrated to a depth of 120 μm : a large number of cells was observed into the entire structure (Fig. 11 B).

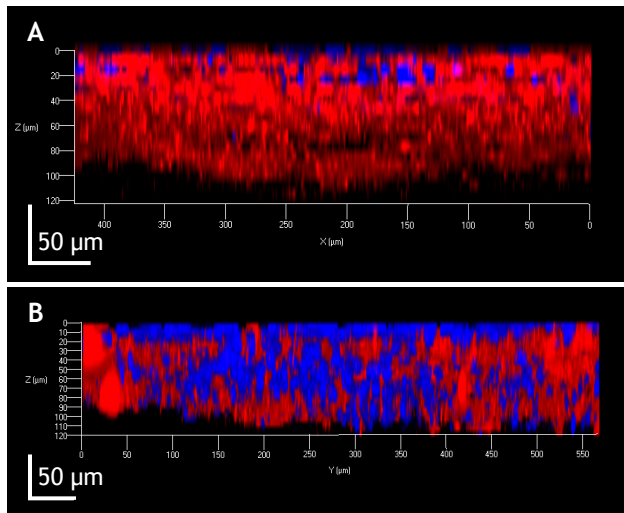


Figure 11: Migration of DPSC through a stack of five PLA/PCL-TA membranes after (A) 14 days and (B) 28 days. Confocal micrographs showed the 3D reconstruction of the stack of membranes from 4 μm Z-stack images. DPSC nuclei were stained in blue with DAPI and PLA fibers were stained with Nile Red.

3.5 Analysis of DPSC proliferation and colonization into the 3D conical scaffolds

Cell proliferation on the cone was assessed by an Alamar blue assay over 30 days (Fig. 12). Cells highly proliferated into the cones after 14 days of culture and finally remained stable until 21 days with no significant difference. Between 21 and 28 days of culture, number of cells significantly decreased.

Cells distribution into the cones was observed with confocal microscopy from histological slides after 7, 14, 21, and 28 days of culture (Fig. 13). Results showed that cells formed a regular

layer on the surface of the cones. They were also well distributed through the walls formed by the layers of the rolled membranes.

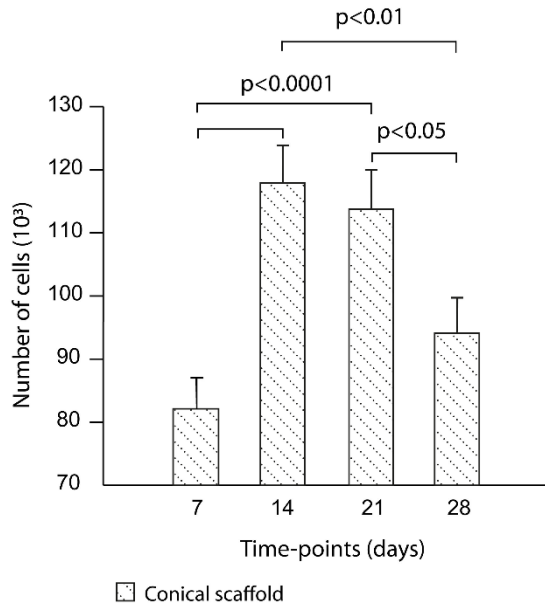


Figure 12: DPSC proliferation into the cone until 1 month. Number of cells was analyzed with an Alamar blue assay after 7, 14, 21 and 28 days. Mean for $n = 3 \pm SD$.

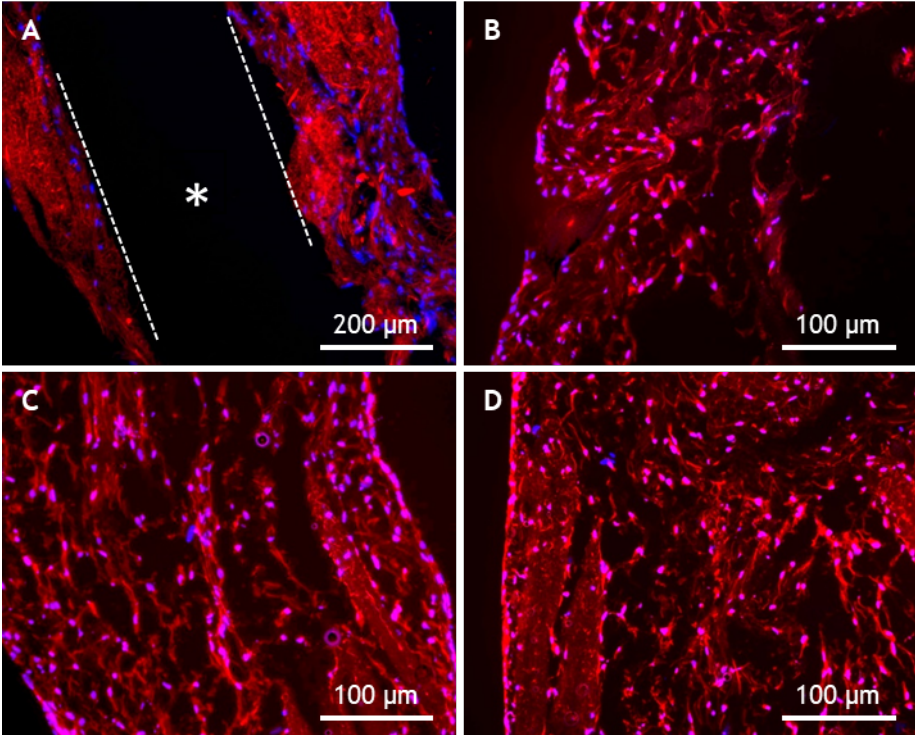


Figure 13: Axial cross sections of a cone showing DPSC dispersion after (A) 7 days, (B) 14 days, (C) 21 days and (D) 28 days of culture. Confocal micrographs showing DPSC nuclei stained in blue with DAPI and PLA fibers stained with Nile Red. (A) *tubular space due to the finger plugger, magnification 10 X and (B-D) magnification 20X.

4. DISCUSSION

Our objective was to develop an innovative biocompatible scaffold which could trigger dental pulp regeneration through a cell-homing process. In our mind, the design and fabrication of such a biomaterial have to meet several challenges: (i) the scaffold could directly fill the root canal of the teeth and (ii) have an optimized architecture to allow endogenous cell colonization and proliferation into the intra-canal space. Several 3D pre-formed conical or tubular scaffolds were reported to be fabricated for direct implantation in the root canal similar to the present expectation. A collagen/alginate composite scaffold mimicking the shape of a gutta-percha point (usually used as sealing material) and easily manipulated has been developed.³⁵ Authors prepared their scaffold into a mold with an imprint of a gutta-percha point. Then, stem cells from the apical papilla (SCAP) were seeded on the composite scaffold and showed good viability, proliferation and differentiation. Advantages of this kind of biocompatible composite are its ease of preparation and implantation into the canal of a tooth. However, the structure was not porous that could result in a lack of cell infiltration and vascularization within the scaffold could be impeded. Differently, Bhargav *et al.* worked on very porous and structured tubes made from PCL enriched with mineral trioxide aggregate (MTA) by 3D printing.³⁶ Scaffold formulation, pore size and distribution, and degradation rate were well studied and optimized via Taguchi's method to allow sufficient DPSC proliferation. Bottino *et al.* also worked on the development of a 3D tubular structure³⁷ made from electrospun PDS supplemented with three antibiotics (metronidazole, ciproflaxin, and minocycline) for directly intracanal drug delivery. The 3D tubular scaffold showed antimicrobial activity *in vitro* into the

infected root canal of dentin slice, and *in vivo* in a dog model with periapical disease after intracanal disinfection and evoked bleeding procedures. In addition, ingrowth of a thin layer of osteodentin-like tissue into the root canal was observed. The two previous tubular scaffolds described were made either with 3D printing or electrospinning and have similarities with the one developed in the present work. Their results are encouraging for the development and qualification of a 3D implantable structure. Nevertheless, their tubular shape only allows implantation in immature teeth with open apex and not in mature teeth. In a previous work of our group, Louvrier *et al.*, proposed a 3D PCL conical scaffold elaborated by jet-spraying (Biomedical Tissues®, Nantes, France) with similar dimensions of a gutta-percha point, as a support for potentially dental pulp regeneration of mature teeth.³⁰ The tip of the cone having the same diameter as the gutta-percha point was suitable to fit mature teeth. Although such 3D cone was able to promote DPSC proliferation and differentiation, cell colonization was mainly observed on the surface due to the small pore size of the scaffold. Now, efforts were focused on the elaboration by electrospinning of a 3D tubular scaffold having larger pores with a conical shape based on the dimension of the gutta-percha point.

To meet the requirements for future clinical use, porous and structured 3D composite membranes with PLA nanofibers and PCL-AT microparticles were first fabricated using the process ETAD. All the process has been optimized for the structured distribution of fibers and particles on the collector. PLA concentration was optimized at 10% in solution and the flow rate was fixed at 1.7 mL/h to have smooth and uniform nanofibers without beads under any temperature and humidity conditions. To obtain structured membranes with large pores, deposition of particles on a microstructure template was necessary. PCL was chosen because it is easily electrospayed. TA was mixed with PCL in the particle to not dissolve too quickly and to remain biocompatible at low concentration. Only with 10% PCL solution and 30% TA (relative to the weight of PCL) particles were well shaped and distributed on the protuberances

of the collector. A low flow rate was needed for the good particles distribution but at that flow rate only few particles were electrosprayed. Therefore to increase particle number, three needles were used. Collection time of the membranes was fixed at 13 min to keep porous areas with low density of fibers for cell penetration. Indeed, as shown by SEM, such strategy led to the fabrication of well-organized membranes having 3D domains being highly porous with a very low density of nanofibers. These domains, poorly dense in fibers, were interconnected by aligned PLA fibers and nodes made of intertwined PLA fibers and PCL-TA microparticles that insure the cohesion of the membranes. In addition, it is expected that the porous domains could ensure stem cell colonization and migration. Then, these membranes were rolled to form 3D conical scaffolds around a finger plugger. Once positioned in the canal, the finger spreader is withdrawn leaving a hollow cone with an inner canal with a maximum end size of 500 μm . As shown by SEM, cross-sections of the cones were circular with several layers of membranes overlaid. Advantages of cone preparation around a finger plugger are twofold: ancillary allows the manipulation of the cone and guidance inside the root canal during implantation. Secondly, it creates an hollow structure that could be favorable for blood penetration and blood clot formation in an evoked bleeding procedure in endodontic.¹

One question pending was the maintenance of void areas from the planar membranes once rolled in the form of a cone. Cones were composed of several layers of stacked planar membranes. To mimic this structure, a stack of 5 layers of plane membranes were used to test cell migration through. After 1 month, results showed that cells could migrate through a thickness of 120 μm from the top to the bottom of the membrane stacks. A large number of cells were observed into the entire volume proving that the designed porous structure of electrospun membranes was favorable for cell migration. Following this validation, cellular colonization and infiltration were tested onto the 3D conical scaffolds. Histological analysis showed that cells colonized the entire volume of cones. A layer of continuous cells was visible

on the external and internal layers of the cone. In addition, it was found that cells were capable of proliferation onto the cones up to 14 days.

PLA and PCL are biocompatible polymers with high structural stability and a slow degradation rate. Degradation of polyester scaffolds can involve local pH variation or loss of scaffold mechanical strength that can affect tissue regeneration. However, the use of these materials is widespread in tissue engineering whereas biodegradability studies of nanofiber scaffolds are limited.³⁸ Only few studies analyzed the degradation of PLLA nanofibers with fiber diameters of 290 or 650 nm without significant degradation after 7 or 14 weeks respectively.^{39,40} Similarly, our results of pH measurements did not show significant *in vitro* degradation of the cones after 120 days. Measurement of weights was uncertain because cones initially weighted less than 1 mg each, leading to measurement errors close to the reliability limit of the balance. However, SEM exploration showed that the structure of the cones has been loosened or even collapsed showing a physical degradation after 120 days. *In vitro* experiment of polymer degradation was conducted as commonly described³⁸ to have first results on degradation rate but this model does not rely on cellular mechanisms *in vivo*. *In vivo* experiments should be conducted to better understand the degradation time of the cone in parallel with tissue formation.

Antimicrobial activity of TA on *E. Coli* and *S. Aureus* and minimum inhibitory concentration (MIC), already confirmed in a previous work, were determined at 105 µg/mL for *E. Coli* and 100 µg/mL for *S. Aureus*.⁴¹ However, TA can also be cytotoxic for cells over a concentration of 200 µg/mL.⁴¹ Quantification of TA released from the cone after several days is mandatory to predict its effects against bacteria and its toxicity. Results showed that the concentration of TA released from the cones was 58 µg/mL (60% of the total concentration detected) after 24 hours and 97 µg/mL after 10 days. The concentration of TA released from the cones was closed to the MIC against *E. Coli* and *S. Aureus* as previously determined. Experiments will be specifically carried out to assess the antimicrobial activity of the cones against major

endodontic bacteria as *E. Faecalis*. Gelatin coating of the cone modify TA release, indeed TA released from PLA/PCL-TA membranes was higher than from G@PLA/PCL-TA membranes on the first day. Gelatin dissolution assay showed that 85% of gelatin was removed after one day, we could therefore assume that it does not longer retained TA after this.

We used gelatin as a stabilizing agent for the cone otherwise we would have faced the uncoiling of the membrane. Gelatin is a biocompatible natural polymer derived from collagen, already used to made scaffolds for regenerative endodontics. Yang *et al.*, made an electrospun scaffold with gelatin, PCL and hydroxyapatite (HA). Results showed that scaffold supported odontogenic differentiation of DPSC *in vivo*, and bone-like matrix formation when seeded with DPSC prior to implantation in nude mice.¹⁹ Another study showed that gelatin hydrogel combined with FGF-2 induced dentin regeneration on amputated pulp.⁴² Gelatin has ability to serve as carrier for bioactive molecule delivery.⁴³⁻⁴⁵ For dental pulp regeneration, gelatin could serve as a reservoir of growth factors that could be released inside the root canal to enhance healing potential. It was found that growth factors as SDF-1 α , bFGF, VEGF or PDGF added to scaffolds can enhance cellular behavior *in vitro* and dental pulp healing in animal models.^{6,15,46} Yang *et al.* showed the potential of SDF-1 α (stromal cell-derived factor) on DPSC migration *in vitro*.⁴⁷ They also demonstrated in an *in vivo* ectopic transplantation model of silk fibroin scaffolds loaded with SDF-1 α that vascularized connectives tissue was formed. Kim *et al.* studied the *in vivo* transplantation (ectopic model in mouse) of collagen scaffolds added with bFGF, VEGF, or PDGF with a basal set of nerve growth factor (NGF) and BMP-7. Newly connective tissue with abundant cells, vascularization, and dentine formation was observed.⁴⁸ These growth factors could be good candidates for the present purpose if needed for further experiments. Aside, in our case, gelatin coating on G@PLA/PCL-TA membranes increased their biocompatibility.

Taken together, all of our results prove that the composition, architecture, 3D shaping, and functionalization of our biomaterial are in favor of cell attachment, proliferation, and colonization, which were essential for tissue regeneration mediated by the cell-homing process.

5. CONCLUSION

This study was focused on the fabrication of a 3D porous conical scaffold dedicated to regenerative endodontics. The cone was designed to fill prepared root canals for its potential use in revascularization procedure. The cone was made from well-structured composite membranes of electrospun PLA nanofibers and electrospayed PCL/TA particles. The cones were coated with gelatin enhancing their integrity in order to facilitate their insertion in the root canal while enhancing DPSC biocompatibility. The well-controlled highly porous architecture of the cone was favorable for infiltration and colonization of DPSC within their entire structure. Such a 3D conical scaffold is a prototype qualified for tissue engineering and adapted to its potential future use in endodontic.

ASSOCIATED CONTENT

Supporting Information:

(1) SEM micrographs of the surface of G@PLA/PCL-TA membranes coated with gelatin. Images showed the degradation of the gelatin layer when immersed in PBS at 37°C for 1 and 7 days.

(2) Study of the cone degradation when immersed in PBS at 37°C for 1, 7 days, 15 and 120 days. Surface of the cones were evidenced by SEM.

AUTHOR INFORMATION

Corresponding Author

Lisa Terranova

Université de Strasbourg, Institut National de la Santé et de la Recherche Médicale, Unité mixte de recherche 1121, Biomaterials and Bioengineering, Strasbourg, France

lisa.terranova@inserm.fr

Author Contributions

The manuscript was written through contributions of all authors. All authors have given approval to the final version of the manuscript.

Funding Sources

This research was supported by Institut Carnot MICA (project ElectrATpulpe) and Agence national de la recherche (ANR), project RooTRaCE (ANR-20-CE19-0008).

ACKNOWLEDGMENT

The authors thanks Eric Mathieu for his help with scanning electron microscopy.

ABBREVIATIONS

PLA, poly (lactic acid); PCL, polycaprolactone; TA, tannic acid; SEM, scanning electron microscopy; DPSC, dental pulp stem cells; MSC, mesenchymal stem cells; TGF- β , transforming growth factor- β ; PDGF, platelet-derived growth factor; bFGF, basic fibroblast growth factor; VEGF, vascular endothelial growth factor; BMP-1, bone morphogenetic protein 1; EDTA, ethylenediamine tetraacetic acid; PDS, polydioxanone; PDL, periodontal ligament stem cells; ETAD, electrostatic template assisted deposition; DCM, dichloromethane; DMF, N,N-dimethylformamide; DMAc, dimethylacetamide; PBS, phosphate-buffered saline ; BCA, bicinchoninic acid; BSA, bovine serum albumin; α -MEM, minimum essential medium, α modification; FBS, fetal bovine serum; TCP, tissue culture

plate; ALP, alkaline phosphatase; PHEMA, polyhydroxyethylmethacrylate; DAPI, 4', 6-diamidino-2-phenylindole; SCAP, stem cells from the apical papilla; MTA, mineral trioxide aggregate; HA, hydroxyapatite; PEO, poly (ethylene oxide); PLLA, poly (L, lactide); MIC, minimum inhibitory concentration; SDF-1 α , stromal cell-derived factor; NGF, nerve growth factor; BMP-7, bone morphogenetic protein 7.

REFERENCES

- (1) Wigler, R.; Kaufman, A. Y.; Lin, S.; Steinbock, N.; Hazan-Molina, H.; Torneck, C. D. Revascularization: A Treatment for Permanent Teeth with Necrotic Pulp and Incomplete Root Development. *J. Endod.* **2013**, *39* (3), 319–326.
- (2) Shimizu, E.; Jong, G.; Partridge, N.; Rosenberg, P. A.; Lin, L. M. Histologic Observation of a Human Immature Permanent Tooth with Irreversible Pulpitis after Revascularization/Regeneration Procedure. *J. Endod.* **2012**, *38* (9), 1293–1297.
- (3) Shah, N.; Logani, A.; Bhaskar, U.; Aggarwal, V. Efficacy of Revascularization to Induce Apexification/Apexogenesis in Infected, Nonvital, Immature Teeth: A Pilot Clinical Study. *J. Endod.* **2008**, *34* (8), 919–925.
- (4) Arslan, H.; Ahmed, H. M. A.; Şahin, Y.; Doğanay Yıldız, E.; Gündoğdu, E. C.; Güven, Y.; Khalilov, R. Regenerative Endodontic Procedures in Necrotic Mature Teeth with Periapical Radiolucencies: A Preliminary Randomized Clinical Study. *J. Endod.* **2019**, *45* (7), 863–872.
- (5) Saoud, T. M.; Martin, G.; Chen, Y.-H. M.; Chen, K.-L.; Chen, C.-A.; Songtrakul, K.; Malek, M.; Sigurdsson, A.; Lin, L. M. Treatment of Mature Permanent Teeth with Necrotic Pulps and Apical Periodontitis Using Regenerative Endodontic Procedures: A Case Series. *J. Endod.* **2016**, *42* (1), 57–65.
- (6) Eramo, S.; Natali, A.; Pinna, R.; Milia, E. Dental Pulp Regeneration *via* Cell Homing. *Int Endod J* **2018**, *51* (4), 405–419.
- (7) Diogenes, A.; Henry, M. A.; Teixeira, F. B.; Hargreaves, K. M. An Update on Clinical Regenerative Endodontics: An Update on Clinical Regenerative Endodontics. *Endod Topics* **2013**, *28* (1), 2–23.
- (8) Liao, J.; Al Shahrani, M.; Al-Habib, M.; Tanaka, T.; Huang, G. T.-J. Cells Isolated from Inflamed Periapical Tissue Express Mesenchymal Stem Cell Markers and Are Highly Osteogenic. *J. Endod.* **2011**, *37* (9), 1217–1224.
- (9) Chrepa, V.; Henry, M. A.; Daniel, B. J.; Diogenes, A. Delivery of Apical Mesenchymal Stem Cells into Root Canals of Mature Teeth. *J. Dent. Res.* **2015**, *94* (12), 1653–1659.
- (10) Smith, J. G.; Smith, A. J.; Shelton, R. M.; Cooper, P. R. Recruitment of Dental Pulp Cells by Dentine and Pulp Extracellular Matrix Components. *Exp. Cell Res.* **2012**, *318* (18), 2397–2406.
- (11) Widbiller, M.; Eidt, A.; Lindner, S. R.; Hiller, K.-A.; Schweikl, H.; Buchalla, W.; Galler, K. M. Dentine Matrix Proteins: Isolation and Effects on Human Pulp Cells. *Int. Endod. J.* **2018**, *51*, e278–e290.
- (12) Galler, K. M.; D'Souza, R. N.; Federlin, M.; Cavender, A. C.; Hartgerink, J. D.; Hecker, S.; Schmalz, G. Dentin Conditioning Codetermines Cell Fate in Regenerative Endodontics. *J. Endod.* **2011**, *37* (11), 1536–1541.
- (13) Galler, K. M.; Widbiller, M. Cell-Free Approaches for Dental Pulp Tissue Engineering. *J. Endod.* **2020**, *46* (9), S143–S149.

- (14) Kim, J. Y.; Xin, X.; Muioli, E. K.; Chung, J.; Lee, C. H.; Chen, M.; Fu, S. Y.; Koch, P. D.; Mao, J. J. Regeneration of Dental-Pulp-like Tissue by Chemotaxis-Induced Cell Homing. *Tissue Eng. Part A* **2010**, *16* (10), 3023–3031.
- (15) Albuquerque, M. T. P.; Valera, M. C.; Nakashima, M.; Nör, J. E.; Bottino, M. C. Tissue-Engineering-Based Strategies for Regenerative Endodontics. *J. Dent. Res.* **2014**, *93* (12), 1222–1231.
- (16) Prescott, R. S.; Alsanea, R.; Fayad, M. I.; Johnson, B. R.; Wenckus, C. S.; Hao, J.; John, A. S.; George, A. In Vivo Generation of Dental Pulp-like Tissue by Using Dental Pulp Stem Cells, a Collagen Scaffold, and Dentin Matrix Protein 1 after Subcutaneous Transplantation in Mice. *J. Endod.* **2008**, *34* (4), 421–426.
- (17) Ma, P. X.; Zhang, R. Synthetic Nano-scale Fibrous Extracellular Matrix. *J. Biomed. Mater. Res.* **1999**, *46*, 60–72.
- (18) Gupte, M. J.; Ma, P. X. Nanofibrous Scaffolds for Dental and Craniofacial Applications. *J. Dent. Res.* **2012**, *91* (3), 227–234.
- (19) Yang, X.; Yang, F.; Walboomers, X. F.; Bian, Z.; Fan, M.; Jansen, J. A. The Performance of Dental Pulp Stem Cells on Nanofibrous PCL/Gelatin/NHA Scaffolds. *J. Biomed. Mater. Res.* **2009**, *9999A*, NA-NA.
- (20) Yun, H.-M.; Kang, S.-K.; Singh, R. K.; Lee, J.-H.; Lee, H.-H.; Park, K.-R.; Yi, J.-K.; Lee, D.-W.; Kim, H.-W.; Kim, E.-C. Magnetic Nanofiber Scaffold-Induced Stimulation of Odontogenesis and pro-Angiogenesis of Human Dental Pulp Cells through Wnt/MAPK/NF-KB Pathways. *Dent. Mater.* **2016**, *32* (11), 1301–1311.
- (21) Zhang, S.; Huang, Y.; Yang, X.; Mei, F.; Ma, Q.; Chen, G.; Ryu, S.; Deng, X. Gelatin Nanofibrous Membrane Fabricated by Electrospinning of Aqueous Gelatin Solution for Guided Tissue Regeneration. *J. Biomed. Mater. Res.* **2009**, *90A* (3), 671–679.
- (22) Yoo, H. S.; Kim, T. G.; Park, T. G. Surface-Functionalized Electrospun Nanofibers for Tissue Engineering and Drug Delivery. *Adv. Drug Deliv. Rev.* **2009**, *61* (12), 1033–1042.
- (23) Bottino, M. C.; Kamocki, K.; Yassen, G. H.; Platt, J. A.; Vail, M. M.; Ehrlich, Y.; Spolnik, K. J.; Gregory, R. L. Bioactive Nanofibrous Scaffolds for Regenerative Endodontics. *J. Dent. Res.* **2013**, *92* (11), 963–969.
- (24) Rnjak-Kovacina, J.; Weiss, A. S. Increasing the Pore Size of Electrospun Scaffolds. *Tissue Eng. Part B: Reviews* **2011**, *17* (5), 365–372.
- (25) Wittmer, C. R.; Hébraud, A.; Nedjari, S.; Schlatter, G. Well-Organized 3D Nanofibrous Composite Constructs Using Cooperative Effects between Electrospinning and Electrospraying. *Polymer* **2014**, *55* (22), 5781–5787.
- (26) Dissanayaka, W. L.; Hargreaves, K. M.; Jin, L.; Samaranyake, L. P.; Zhang, C. The Interplay of Dental Pulp Stem Cells and Endothelial Cells in an Injectable Peptide Hydrogel on Angiogenesis and Pulp Regeneration *In Vivo*. *Tissue Eng. Part A* **2015**, *21* (3–4), 550–563.
- (27) Dobie, K.; Smith, G.; Sloan, A. J.; Smith, A. J. Effects of Alginate Hydrogels and TGF-Beta 1 on Human Dental Pulp Repair in Vitro. *Connect Tissue Res.* **2002**, *43* (2–3), 387–390.
- (28) Galler, K. M.; Hartgerink, J. D.; Cavender, A. C.; Schmalz, G.; D’Souza, R. N. A Customized Self-Assembling Peptide Hydrogel for Dental Pulp Tissue Engineering. *Tissue Eng. Part A* **2012**, *18* (1–2), 176–184.
- (29) Bottino, M. C.; Yassen, G. H.; Platt, J. A.; Labban, N.; Windsor, L. J.; Spolnik, K. J.; Bressiani, A. H. A. A Novel Three-Dimensional Scaffold for Regenerative Endodontics: Materials and Biological Characterizations: 3D Scaffold for Regenerative Endodontics. *J. Tissue Eng. Regen. Med.* **2013**, *9* (11), E116–E123.
- (30) Louvrier, A.; Euvrard, E.; Nicod, L.; Rolin, G.; Gindraux, F.; Pazart, L.; Houdayer, C.; Risold, P. Y.; Meyer, F.; Meyer, C. Odontoblastic Differentiation of Dental Pulp Stem

- Cells from Healthy and Carious Teeth on an Original PCL-Based 3D Scaffold. *Int. Endod. J.* **2018**, *51*, e252–e263.
- (31) Kaczmarek, B. Tannic Acid with Antiviral and Antibacterial Activity as A Promising Component of Biomaterials—A Minireview. *Materials* **2020**, *13* (14), 3224.
 - (32) Sahiner, N.; Sagbas, S.; Aktas, N. Single Step Natural Poly(Tannic Acid) Particle Preparation as Multitalented Biomaterial. *Mater. Sci. Eng. C* **2015**, *49*, 824–834.
 - (33) Mailley, D.; Hébraud, A.; Schlatter, G. A Review on the Impact of Humidity during Electrospinning: From the Nanofiber Structure Engineering to the Applications. *Macromol. Mater. Eng.* **2021**, *306* (7), 2100115.
 - (34) Wang, J.; Ma, H.; Jin, X.; Hu, J.; Liu, X.; Ni, L.; Ma, P. X. The Effect of Scaffold Architecture on Odontogenic Differentiation of Human Dental Pulp Stem Cells. *Biomaterials* **2011**, *32* (31), 7822–7830.
 - (35) Devillard, R.; Rémy, M.; Kalisky, J.; Bourget, J.-M.; Kérourédan, O.; Siadous, R.; Bareille, R.; Amédée-Vilamitjana, J.; Chassande, O.; Fricain, J.-C. *In Vitro* Assessment of a Collagen/Alginate Composite Scaffold for Regenerative Endodontics. *Int. Endod. J.* **2017**, *50* (1), 48–57.
 - (36) Bhargav, A.; Min, K.; Wen Feng, L.; Fuh, J. Y. H.; Rosa, V. Taguchi's Methods to Optimize the Properties and Bioactivity of 3D Printed Polycaprolactone/Mineral Trioxide Aggregate Scaffold: Theoretical Predictions and Experimental Validation. *J. Biomed. Mater. Res.* **2019**, jbm.b.34417.
 - (37) Bottino, M. C.; Albuquerque, M. T. P.; Azabi, A.; Münchow, E. A.; Spolnik, K. J.; Nör, J. E.; Edwards, P. C. A Novel Patient-specific Three-dimensional Drug Delivery Construct for Regenerative Endodontics. *J. Biomed. Mater. Res.* **2019**, *107* (5), 1576–1586.
 - (38) Dong, Y.; Liao, S.; Ngiam, M.; Chan, C. K.; Ramakrishna, S. Degradation Behaviors of Electrospun Resorbable Polyester Nanofibers. *Tissue Eng. Part B Rev.* **2009**, *15* (3), 333–351.
 - (39) Bhattarai, S. R.; Bhattarai, N.; Viswanathamurthi, P.; Yi, H. K.; Hwang, P. H.; Kim, H. Y. Hydrophilic Nanofibrous Structure of Polylactide; Fabrication and Cell Affinity. *J. Biomed. Mater. Res.* **2006**, *78A* (2), 247–257.
 - (40) You, Y.; Min, B.-M.; Lee, S. J.; Lee, T. S.; Park, W. H. In Vitro Degradation Behavior of Electrospun Polyglycolide, Polylactide, and Poly(Lactide-Co-Glycolide). *J. Appl. Polym. Sci.* **2005**, *95* (2), 193–200.
 - (41) Reitzer, F.; Berber, E.; Halgand, J.; Ball, V.; Meyer, F. Use of Gelatin as Tannic Acid Carrier for Its Sustained Local Delivery. *Pharm. Front.* **2020**, *2* (1).
 - (42) Ishimatsu, H.; Kitamura, C.; Morotomi, T.; Tabata, Y.; Nishihara, T.; Chen, K.-K.; Terashita, M. Formation of Dentinal Bridge on Surface of Regenerated Dental Pulp in Dentin Defects by Controlled Release of Fibroblast Growth Factor-2 From Gelatin Hydrogels. *J. Endod.* **2009**, *35* (6), 858–865.
 - (43) Young, S.; Wong, M.; Tabata, Y.; Mikos, A. G. Gelatin as a Delivery Vehicle for the Controlled Release of Bioactive Molecules. *J. Control. Release* **2005**, *109* (1–3), 256–274.
 - (44) Yamamoto, M.; Ikada, Y.; Tabata, Y. Controlled Release of Growth Factors Based on Biodegradation of Gelatin Hydrogel. *J. Biomater. Sci. Ed. Polym.* **2001**, *12* (1), 77–88.
 - (45) Santoro, M.; Tatara, A. M.; Mikos, A. G. Gelatin Carriers for Drug and Cell Delivery in Tissue Engineering. *Journal of Controlled Release* **2014**, *190*, 210–218.
 - (46) Yang, J.; Yuan, G.; Chen, Z. Pulp Regeneration: Current Approaches and Future Challenges. *Front. Physiol.* **2016**, *7*.

- (47) Yang, J.; Zhang, Y.; Wan, C.; Sun, Z.; Nie, S.; Jian, S.; Zhang, L.; Song, G.; Chen, Z. Autophagy in SDF-1 α -Mediated DPSC Migration and Pulp Regeneration. *Biomaterials* **2015**, *44*, 11–23.
- (48) Kim, J. Y.; Xin, X.; Moioli, E. K.; Chung, J.; Lee, C. H.; Chen, M.; Fu, S. Y.; Koch, P. D.; Mao, J. J. Regeneration of Dental-Pulp-like Tissue by Chemotaxis-Induced Cell Homing. *Tissue Eng. Part A* **2010**, *16* (10), 3023–3031.